# Efficient Estimation of Sensitivities for Counterparty Credit Risk with the Finite Difference Monte Carlo Method

de Graaf, C.S.L.; Kandhai, D.; Sloot, P.M.A.

**DOI**
10.2139/ssrn.2521431
10.21314/JCF.2016.325

**Publication date**
2017

**Document Version**
Submitted manuscript

**Published in**
Journal of Computational Finance

# Efficient Estimation of Sensitivities for Counterparty Credit Risk with the Finite Difference Monte-Carlo Method

Cornelis S. L. de Graaf*[a], Drona Kandhai[a,b] and Peter M.A. Sloot[a,c,d]

[a]Computational Science, University of Amsterdam, Amsterdam, the Netherlands
[b]Quantitative Analytics, ING Bank, Amsterdam, the Netherlands
[c]National Research University ITMO, St. Petersburg, Russia
[d]Complexity Institute, Nanyang Technological University, Singapore

December 16, 2014

**Abstract**

According to Basel III, financial institutions have to charge a *Credit Valuation Adjustment* (CVA) to account for a possible counterparty default. Calculating this measure and its sensitivities is one of the big challenges in risk management. Here we introduce an efficient method for the estimation of CVA and its sensitivities for a portfolio of financial derivatives. We use the *Finite Difference Monte-Carlo* (FDMC) method to measure exposure profiles and consider the computationally challenging case of FX barrier options in the context of the Black-Scholes as well as the Heston Stochastic Volatility model for a wide range of parameters. Our results show that FDMC is an accurate method compared to the semi-analytic COS method and has as an advantage that it can compute multiple options on one grid, which paves the way for real portfolio level risk analysis.

*keywords:* Finite Difference-Monte Carlo, Credit Valuation Adjustment, Barrier options, Portfolio.

## 1 Introduction

Financial crises typically have various causes, but often have one effect: the call to model more risk factors. Since 1987, it is known that the volatility used in option pricing is not constant and can better be modeled as a stochastic

*Corresponding author. E-mail address: C.S.L.deGraaf@uva.nl.

process itself (Heston (1993)). More recently, since the Lehman collapse in 2008, measures are taken to prevent losing money from a worthless derivative due to counterparty default. Currently, a single price of an option or financial derivative is therefore not sufficient, institutions also need to know the creditworthiness of their counterparty.

Regulators drafted the Basel III accords (Basel Committee on Banking Supervision (2010)) which announced that banks need to charge a premium to their trading counterparty for its creditworthiness. This is done via the so-called *Credit Valuation Adjustment* (CVA) that adjusts the price of a derivative according to the creditworthiness of the counterparty. Moreover, additional capital requirements and limit monitoring based on potential future losses should be in place. Computing these measures implies that valuation and risk management of even straightforward plain vanilla options already becomes a high dimensional and complex problem.

In de Graaf et al. (2014) we introduced the *Finite Difference Monte Carlo* (FDMC) method to calculate the exposure profiles of a derivative. This is done for Bermudan put options which have an early exercise feature at preset discrete time points. Similar as in Ng and Peterson (2009) and Ng et al. (2010), the FDMC method uses the scenario generation from the Monte Carlo method. Option prices are computed on a grid with the finite difference method and option values per path are obtained by interpolation on this grid. The Expected Exposure (EE) equals mean of the resulting option price distribution whereas the Potential Future Exposure (PFE) is a quantile of this distribution. In practice, apart from EE and PFE, the sensitivities to market factors (like spot value, interest rate and volatility) are required for hedging and control of the CCR of derivatives portfolios.

In this paper we extend our previous study and consider the estimation of first and second-order sensitivities. In contrast to the widely used bump-and-revalue method, we propose a path dependent estimator that is leveraging from the already estimated local sensitivities on the finite difference grid. A rigorous analysis is performed in the case of barrier options which pose severe numerical challenges due to the knock-out feature that results in a discontinuous terminal condition. Similar discontinuities also arise in portfolios with instruments of different maturities, with the possibility of error propagation on the computation grid in time. Therefore we analyze such portfolios specifically in this work. Apart from these numerical difficulties, we further incorporate the highly relevant skew effect which is dominantly present in the *Foreign Exchange* (FX) market. The Heston model is therefore chosen to drive the underlying FX rate and plain vanilla and barrier options on FX rates are considered. As a benchmark we use the Monte Carlo COS method (Shen et al. (2013)).

The outline of this paper is as follows. In section 2 we describe CVA and its sensitivity with respect to the initial underlying value. Section 3 will be the core of this research where we describe the FDMC method together with the adjustments to measure the sensitivity of CVA and how to extend to handle multiple options. In section 4 we present results for a number of test problems and in section 5 the conclusions are summarized.

# 2 Problem Formulation

## 2.1 CVA under Heston's Stochastic Volatility Model

In the Heston model, the volatility is modeled as a stochastic process such that the volatility smile can be captured. The two-dimensional dynamics are given by:

$$\begin{aligned} dS_t &= (r^d - r^f)S_t dt + \sqrt{V_t} S_t dW_t^1, \\ dV_t &= \kappa(\eta - V_t)dt + \sigma\sqrt{V_t} dW_t^2, \\ dW_t^1 dW_t^2 &= \rho dt, \end{aligned} \tag{1}$$

where $r^d$ ($r^f$) is the domestic (foreign) interest rate, $\kappa$ the mean-reverting speed in the Cox-Ingersoll-Ross (CIR) process for the variance, $\eta$ the level of the long term mean, $\sigma$ the so-called volatility of volatility and $W_t^1$ and $W_t^2$ are two Wiener processes with correlation $\rho$. The price $U$ of an option with maturity $T$, payoff function $\phi(S_T, V_T)$ and with the initial value of the underlying and volatility equal to $S$ and $V$ respectively equals:

$$U(S, V, t) = \mathbb{E}\left[\mathrm{e}^{-r^d(T-t)}\phi(S_T, V_T)|S_0 = S, V_0 = V\right]. \tag{2}$$

Because of the stochastic volatility component, pricing formula's are two dimensional and an analytic option price is harder to obtain, or not available. This is why numerical techniques, like the Monte Carlo method or the finite difference method to solve the associated PDE, are employed.

For risk purposes it is obvious that one is interested in the case that a loss is positive (a negative loss may be a profit), therefore the exposure of an option at a future time $t < T$ is defined as:

$$\mathrm{E}(t) := \max(U(S_t, V_t, t), 0), \tag{3}$$

where $U(S_t, V_t, t)$ is the (mark-to-market) value of a financial derivatives contract at time $t$.

The present Expected Exposure (EE) at a future time $t < T$ is given by:

$$\mathrm{EE}(t) := \mathbb{E}\left[\mathrm{E}(t)|\mathcal{F}_0\right], \tag{4}$$

where $\mathcal{F}_0$ is the filtration at time $t = 0$. In this research, the expectation is calculated under risk-neutral measure $\mathbb{Q}$ [1]. In the case of a long position in a call or put option, the price (2) is always positive and thus the EE (4) is equal to the future option price.

Another important risk assessment is given by the PFE. The quantiles $\theta = 97.5\%$ and $\theta = 2.5\%$ of the exposure distribution at time $t$, are defined as

$$\mathrm{PFE}_\theta(t) = \inf\{x : \mathbb{P}(\mathrm{EE}(t) \le x) \ge \theta\}. \tag{5}$$

While computing CVA, we assume that the exposure and the counterparties default probability are independent. Next to that, as in the Heston model the

[1]Typically, the future states can also be modeled under real-world measure $\mathbb{P}$. This is possible when the FDMC method is used, but as this research focuses on the numerical applicability of this method, the risk-neutral measure $\mathbb{Q}$ is assumed.

discount factor is a deterministic function of time and short rate, the discount factor is also independent of the exposure. The more general case, when the interest rate is assumed to be stochastic, is analyzed in Appendix A. In the case of independence between discount factor, exposure and default probability, we can formulate the expression for credit valuation adjustment (CVA) as follows (Gregory (2010)):

$$\mathrm{CVA}(0,T) = (1-R)\int_0^T D(0,t)\mathrm{EE}(t)dPD(t), \tag{6}$$

where $R$ is the recovery rate, $D(0,t)$ is the risk-free discount factor and $PD(t)$ denotes the default probability of the counterparty at time $t$. The three essential elements are thus: recovery rate, EE and default probability.

In practice CVA is hedged and thus practitioners compute the sensitivity of the CVA with respect to the underlying. We assume that the default probability is independent of exposure and that the discount factor is independent of the spot, such that the sensitivity with respect to $S_0$ can be rewritten as:

$$\begin{aligned}\frac{\partial \mathrm{CVA}(T)}{\partial S_0} &= \frac{\partial}{\partial S_0}\left((1-R)\int_0^T D(0,t)\mathrm{EE}(t)dPD(t)\right),\\ &= (1-R)\int_0^T D(0,t)\frac{\partial \mathrm{EE}(t)}{\partial S_0}dPD(t).\end{aligned} \tag{7}$$

Following the same arguments, the second derivative with respect to $S_0$ can be computed as:

$$\begin{aligned}\frac{\partial^2 \mathrm{CVA}(T)}{\partial S_0^2} &= \frac{\partial}{\partial S_0}\left((1-R)\int_0^T D(0,t)\frac{\partial \mathrm{EE}(t)}{\partial S_0}dPD(t)\right),\\ &= (1-R)\int_0^T D(0,t)\frac{\partial^2 \mathrm{EE}(t)}{\partial S_0^2}dPD(t).\end{aligned} \tag{8}$$

By computing these sensitivities in this way, we need an efficient computation of the derivatives $\frac{\partial \mathrm{EE}(t)}{\partial S_0}$ and $\frac{\partial^2 \mathrm{EE}(t)}{\partial S_0^2}$ for every $t \in [t_0, T]$.

To conclude, the CVA of a portfolio is determined by all the future mark-to-Market (MtM) values of all the options in the portfolio (Basel Committee on Banking Supervision (2010)). If we furthermore want to compute the sensitivities, we also need the derivative at all future market scenarios. These requirements call for a valuation method that can compute option prices and derivatives for a wide range of market scenarios. In this paper we will show that the FDMC method can compute these quantities fast and accurate.

# 3 Computation of Counterparty Exposure and Sensitivities

## 3.1 The FDMC Method

As presented in de Graaf et al. (2014), the *Finite Difference Monte Carlo* (FDMC) method uses the scenario generation of the Monte Carlo method and the pricing approach of the finite difference method. The market states are simulated by the Quadratic Exponential (QE) scheme (Andersen (2008)). Next, a grid in $S$- and $V$-direction is created. This grid is chosen to be sufficiently large to capture all attained values of $S$ and $V$ by the scenario generation. On this grid, prices at any simulation date are calculated by the finite difference procedure. For all simulated market states $(S_m, V_m, t)$ at any time $t$, option prices can be obtained by interpolation on this grid. Specific state $(S_m, V_m, t)$ is interpolated on the grid to obtain option price $U(S_m, V_m, t)$ at each path, for each time point.

At every time point the resulting exposure values for all paths generate a distribution and from this distribution the exposure profiles can be calculated. The EE can be obtained by averaging over all the prices at all the time points. The higher (97.5%) and lower (2.5%) PFE can be computed by taking quantiles.

In the case of a path-dependent barrier option, if the underlying state hits the barrier level $B$, the option is exercised at this path and the exposure for later time points is set to zero. The essential technique of modeling the exposure by the FDMC method can be presented as follows:

- Generate scenarios/paths by Monte Carlo simulation;
- Calculate option values and for barrier options, check which paths hit the barrier.
- Set the exposure at each path as the option value if the option is not exercised; otherwise the exposure and all future exposures of this path are set equal to 0;
- Compute the empirical distribution of the exposure at each exercise time;
- Calculate EE, $\text{PFE}_{2.5\%}$ and $\text{PFE}_{97.5\%}$.

### 3.2 The finite-difference method

For a European option with maturity $T$ and payoff function $\phi$ its risk-neutral value $U$ at $t \leq T$ can be expressed using the conditional expectation under the risk-neutral measure $\mathbb{Q}$ as follows:

$$U(S_{t_0}, V_{t_0}, t_0) = \mathrm{e}^{-r^d(T-t_0)}\mathbb{E}\left[\phi(S_T)\right], \tag{9}$$

where $\phi(\cdot)$ is the payoff function of the option. The finite difference procedure computes the price backward in time starting at maturity $t = T$ back to $t = t_0$. Thus, the pricing function $\nu$ is defined as a function of $\tau = T - t$ such that $\nu(S_\tau, V_\tau, \tau) = U(S_{T-t}, V_{T-t}, T-t)$. The Feynman-Kac theorem links the expectation (9) to the solution of a PDE by no arbitrage arguments, resulting in the following PDE:

$$\frac{\partial \nu}{\partial \tau} = \mathsf{A}\nu, \tag{10}$$

where in the case of an FX option driven by Heston's dynamics, the spatial differential operator $\mathsf{A}$ is given by

$$\begin{aligned}\mathsf{A}\nu =&\frac{1}{2}\sigma^2 V\frac{\partial^2\nu}{\partial V^2}+\rho\sigma VS\frac{\partial^2\nu}{\partial S\partial V}+\frac{1}{2}VS^2\frac{\partial^2\nu}{\partial S^2}\\&+(\kappa[\eta-V])\frac{\partial\nu}{\partial V}+(r^d-r^f)S\frac{\partial\nu}{\partial S}-r^d\nu.\end{aligned}\tag{11}$$

For a given state $(S_{\tau_0}, V_{\tau_0})$ at expiry, the payoff is known. For a down-and-Out barrier call or put option on an underlying $S_{\tau_0}$ with strike $K$ and barrier $B$ this is equal to:

$$\phi(S_{\tau_0}) = \max(\gamma(S_{\tau_0}-K),0)\mathbb{1}_{\{S_{\tau_0}>B\}} \quad \text{with} \quad \gamma = \begin{cases}1, & \text{for a call,}\\ -1, & \text{for a put.}\end{cases}\tag{12}$$

The payoff function for European options can be obtained from this by setting $B = 0$.

### 3.2.1 Space discretization

In the finite difference method this PDE is solved on a finite set of points, by discretizing in $S$- and $V$-direction. The domain to be discretized is chosen as $[0, S_{\max}] \times [0, V_{\max}]$, where $S_{\max}$ and $V_{\max}$ are chosen sufficiently large to minimize the effect of the imposed boundary conditions, but still larger than the largest simulated market scenarios.

Let $s_0 < s_1 < \ldots < s_{m_1}$ and $v_0 < v_1 < \ldots < v_{m_2}$ be the discretization in $S$- and $V$-direction respectively, similar as in Haentjens and in 't Hout (2012). In both dimensions the grid is chosen to be non-uniform. The $S$ dimension consists of a predefined interval $[S_{\text{left}}, S_{\text{right}}]$ in which points are uniformly spaced. $S_{\text{left}}$ and $S_{\text{right}}$ are chosen to contain the region of interest ie, the region around the expected mean of the underlying. Following Haentjens and in 't Hout (2012), for options without barriers we choose:

$$[S_{\text{left}}, S_{\text{right}}] = [0.5K, K]\,.$$

Outside $[S_{\text{left}}, S_{\text{right}}]$, the points are distributed with the help of a sinus hyperbolicus function. In the barrier case, the non-uniform grid is chosen such that the dense region contains more than 95% of the non-exercised paths, generally, choosing

$$[S_{\text{left}}, S_{\text{right}}] = \begin{cases}[0.5K, B]\,, & \text{for a up-and-out call or put,}\\ [B, 1.5K]\,, & \text{for a down-and-out call or put,}\end{cases}$$

is found to be sufficient. For a portfolio of options however, we define $S_{\text{left}}$ and $S_{\text{right}}$ such that all possible strikes and barriers are included.

In $V$-direction the grid is chosen similar as in in 't Hout and Foulon (2010). The grid is dense around $V = 0$. We do this because, for realistic test parameters, the expected mean of the variance process is close to zero and secondly, because the Heston PDE in $V$-direction is convection-dominated close to zero and the initial condition is non-smooth, numerical stability requires a high density of points in this region (Haentjens and in 't Hout (2012)).

The derivatives are approximated using central, forward and backward three point stencils. All stencils are second-order accurate. For more details we refer to Haentjens and in 't Hout (2012).

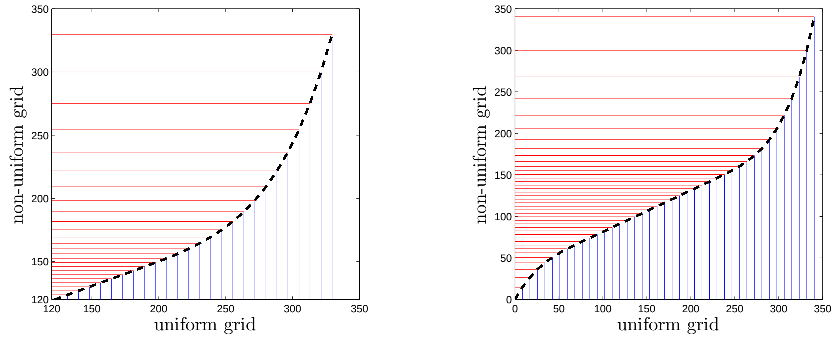


(a) $S$ grid for a DOP option

(b) $S$ grid for a portfolio

Figure 1: Non uniform grids in $S$-direction for a Down-and-Out Put (DOP) option (a) (where we choose $S_{\text{left}} = B = 120$ and $S_{\text{right}} = 140$) and for a portfolio of options (b) (with discontinuous points within $S_{\text{left}} = 100$ and $S_{\text{right}} = 150$).

Table 1: Boundary conditions and payoff functions under the Black-Scholes dynamics.

| Option type | $S \to S_{\max}$ | $S \to S_{\min}$ |
|---|---|---|
| European Call | $\frac{\partial \nu}{\partial S} = 1$ | $\nu = 0$ |
| European Put | $\nu = 0$ | $u = \mathrm{e}^{-r^d(\tau-\tau_0)} K_P$ |
| Up-and-out Barrier Call | $\nu = 0$ | $\nu = 0$ |
| Up-and-out Barrier put | $\nu = 0$ | $\nu = \mathrm{e}^{-r^d(\tau-\tau_0)} K_P$ |
| Down-and-out Barrier Call | $\frac{\partial \nu}{\partial S} = 1$ | $\nu = 0$ |
| Down-and-out Barrier put | $\nu = 0$ | $\nu = 0$ |

### 3.2.2 Boundary conditions

The options considered in this research are of the following type: European call and put options with strike $K_C$ and $K_P$ respectively and barrier options with strike $K_B$ and barrier level $B$, which can be down-and-out or up-and-out calls or puts. The boundary conditions for the $S$ domain used in this research are stated in table 1. Note that in the case of non barrier options, the $S_{\min}$ and $S_{\max}$ converge to 0 or $\infty$ respectively.

The boundary conditions in the volatility direction are imposed independent of the option type. In Ekström and Tysk (2011) it is shown that for a CIR process, like the variance process in the Heston model, the solution to the PDE satisfies the boundary condition that is obtained by inserting $V = 0$ into (11), also referred to as a degenerated boundary condition:

$$\frac{\partial \nu}{\partial \tau} = \kappa \eta \frac{\partial \nu}{\partial V} + (r^d - r^f) S \frac{\partial \nu}{\partial S} - r^d \nu. \tag{13}$$

In traditional literature (see eg, Tavella and Randall (2000)), the maximum variance boundary for call options is imposed as $\nu(S, V_{\max}, \tau) = S$, but experiments show that this introduces a boundary layer. In combination with the PDE becoming convection-dominated around $V \approx 0$ this can result in oscillations if no upwinding is applied. To prevent this problem and still use central schemes, the option value at this boundary is assumed to satisfy $\frac{\partial^2 \nu}{\partial V^2} = 0$.

Using these discretizations, boundary conditions and initial condition, the following initial value problem for stiff *Ordinary Differential Equations* (ODEs) is derived:

$$\begin{cases} \boldsymbol{u}'(\tau) = \mathbf{A}\boldsymbol{u}(\tau) + \boldsymbol{g}(\tau), \\ \boldsymbol{u}(\tau_0) = \phi(\boldsymbol{s}(T)), \end{cases} \tag{14}$$

where $\boldsymbol{u}(\tau)$ denotes the vector of discrete solutions $\boldsymbol{u}_{i,j}(\tau) := u(s_i, v_j, \tau)$ ordered lexicographically, $\boldsymbol{g}(\tau)$ is a vector determined by the boundary conditions and $\boldsymbol{s}(T)$ denotes the grid in $S$-direction at maturity.

### 3.2.3 Time discretization

As the Heston model is a two dimensional problem in space, the ODEs also have two space dimensions. To solve problems with higher dimensions, splitting techniques are relevant. The splitting scheme used this research is the Hundsdorfer-Verwer scheme. For more details we refer to Hundsdorfer and Verwer (2003) for the derivation of the scheme and to in 't Hout and Welfert (2009) for a more detailed explanation of the *Alternating Direction Implicit* (ADI) schemes in this context.

## 3.3 Computing CVA and its Sensitivities

To estimate CVA, we need EE$(t)$ at any time $t \in [t_0, T]$ during the life of the derivative. Next to that we need the probability of default at any time. Following Gregory (2010), we define $q_i = q(t_{i-1}, t_i)$ as the probability that the counterparty will default in the interval $[t - dt, t]$. Using the so-called hazard rate $\lambda_{\text{haz}}$ the survival probability $P_{\text{surv}}(t)$ is defined as:

$$P_{\text{surv}}(t) := \mathrm{e}^{-\lambda_{\text{haz}} t}. \tag{15}$$

Using this definition we can derive the probability to default in interval $(t - dt, t)$ conditioned on no prior default as follows:

$$q(t - dt, t) = P_{\text{surv}}(t) - P_{\text{surv}}(t - dt). \tag{16}$$

For any counterparty for which you can buy a *Credit Default Swap* (CDS) for protection, this entity can be calculated from the CDS spread. As shown in Whetten et al. (2004), the annual premium payment $c$ of a CDS can be calculated as:

$$c = \frac{(1 - R)\sum_{i=1}^{N} P(t_0, t_i)(q_{i-1} - q_i)}{\sum_{i=1}^{N} P(t_0, t_i) q_i dt + \sum_{i=1}^{N} P(t_0, t_i)(q_{i-1} - q_i)\frac{dt}{2}}, \tag{17}$$

where $dt$ denotes the payment interval. In this research we assume annual premiums of 400 basis points, which corresponds to a hazard rate of $6.6 \cdot 10^{-2}$. Now, in a discrete setting, CVA can be calculated as:

$$\text{CVA} = (1 - R)\sum_{k=1}^{N} D(0, t_k) q(t_{k-1}, t_k)\text{EE}(t_k). \tag{18}$$

By using this expression, the first and second derivative of the CVA with respect to the underlying $S_0$ can be derived as follows:

$$\frac{\partial \text{CVA}}{\partial S_0} = \frac{\partial}{\partial S_0}(1-R)\sum_{k=1}^{N} D(0,t_k)q(t_{k-1},t_k)\text{EE}(t_k), \tag{19}$$

$$= (1-R)\sum_{k=1}^{N} D(0,t_k)q(t_{k-1},t_k)\frac{\partial \text{EE}(t_k)}{\partial S_0}, \tag{20}$$

where in the second equality we assume independence between default probability and $S_0$ and loss given default $R$ and $S_0$. Similar, for the second derivative, we have

$$\frac{\partial^2 \text{CVA}}{\partial S_0^2} = (1-R)\sum_{k=1}^{N} D(0,t_k)q(t_{k-1},t_k)\frac{\partial^2 \text{EE}(t_k)}{\partial S_0^2}, \tag{21}$$

To compute $\frac{\partial \text{EE}(t)}{\partial S_0}$ in 20, first, the derivative is rewritten as follows:

$$\frac{\partial \text{EE}(t)}{\partial S_0} = \frac{\partial \text{EE}}{\partial S_t}\frac{\partial S_t}{\partial S_0} + \frac{\partial \text{EE}}{\partial V_t}\frac{\partial V_t}{\partial S_0}, \tag{22}$$

$$= \frac{\partial \text{EE}}{\partial S_t}\frac{\partial S_t}{\partial S_0}. \tag{23}$$

As all considered options have a payoff function depending only on the level of the underlying, the EE is independent of the variance, hence $\frac{\partial V_t}{\partial S_0} = 0$. At every intermediate time point $t_n$, the finite difference method stores the prices for the entire grid in the vector $\boldsymbol{u}^n = \boldsymbol{u}(t_n) = \text{EE}(t_n)$. On this grid we can approximate $\frac{\partial U(t_n)}{\partial S}$ by multiplying with the difference matrix $\mathbf{A}_S$ defined as follows:

$$\frac{\partial \boldsymbol{u}(t_n)}{\partial S} \approx \mathbf{A}_S \boldsymbol{u}^n = \frac{\partial \boldsymbol{u}(t_n)}{\partial S} + \mathcal{O}(\Delta s^2). \tag{24}$$

Next to that, $\frac{\partial S_t}{\partial S_0}$ can be computed by the pathwise Monte Carlo method. Because in the Heston model, the price process follows a Geometric Brownian Motion (GBM), we can assume:

$$S_t = S_0 \mathrm{e}^{(r^d - r^f - \frac{V(t)}{2})t + \sqrt{V(t)}\sqrt{t}Z}, \tag{25}$$

where $Z$ is a standard normal random variable. Consequently, following (Broadie and Glasserman (1996)), for the first and second derivative, we have:

$$\frac{\partial S_t}{\partial S_0} = \mathrm{e}^{(r^d - r^f - \frac{V(t)}{2})t + \sqrt{V(t)}\sqrt{t}Z} = \frac{S_t}{S_0}, \tag{26}$$

$$\frac{\partial^2 S_t}{\partial S_0^2} = 0. \tag{27}$$

Now, at any time point $t_n$ both partial derivatives from (23) can be computed for every path, such that $\frac{\partial \text{EE}(t)}{\partial S_0}$ is obtained by averaging.

To compute (21), we need $\frac{\partial^2 \text{EE}(t)}{\partial S_0^2}$, this yields:

$$
\begin{aligned}
\frac{\partial^2 \text{EE}(t)}{\partial S_0^2} &= \frac{\partial}{\partial S_0}\left(\frac{\partial \text{EE}(t)}{\partial S_{t^*}}\frac{\partial S_{t^*}}{\partial S_0}\right), && (28)\\
&= \left(\frac{\partial}{\partial S_0}\frac{\partial \text{EE}(t)}{\partial S_{t^*}}\right)\frac{\partial S_{t^*}}{\partial S_0} + \frac{\partial \text{EE}(t)}{\partial S_{t^*}}\left(\frac{\partial}{\partial S_0}\frac{\partial S_{t^*}}{\partial S_0}\right), && (29)\\
&= \left(\frac{\partial^2 \text{EE}(t)}{\partial S_{t^*}^2}\frac{\partial S_{t^*}}{\partial S_0}\right)\frac{\partial S_{t^*}}{\partial S_0} + \frac{\partial \text{EE}(t)}{\partial S_{t^*}}\frac{\partial^2 S_{t^*}}{\partial S_0^2}, && (30)\\
&= \frac{\partial^2 \text{EE}(t)}{\partial S_{t^*}^2}\left(\frac{S_{t^*}}{S_0}\right)^2. && (31)
\end{aligned}
$$

Thus, we need the second derivative of EE with respect to $S_{t^*}$, which can also be obtained from the finite difference grid directly.

Similar as in the case of EE, the computation of the first and second derivative can be summarized as follows:

- Generating scenarios/paths by Monte Carlo simulation;
- At each time point $t^*$, for the entire grid, calculate option sensitivities $\frac{\partial \text{EE}(t)}{\partial S_0}$ and $\frac{\partial^2 \text{EE}}{\partial S_0^2}$ for barrier options, check if option is not exercised ($S_{t^*} < B$).
- Set the first and second derivative at each path as the calculated sensitivities if the option is not exercised; otherwise set them equal to 0;
- Compute the empirical distribution of the sensitivities at each exercise time;
- Calculate $\frac{\partial \text{EE}}{\partial S_0}$ and $\frac{\partial^2 \text{EE}}{\partial S_0^2}$ by averaging.

Although we only present results for the two-dimensional Heston model, results hold in a more general sense, for example in the case of stochastic interest rate, the above derivation can be adjusted accordingly as shown in Appendix A.

## 3.4 Pricing a Portfolio

In this research, the finite difference grid is used to price multiple options with different strikes and maturities in one sweep on one grid. The portfolios considered here are constructed of European options and a first order exotic barrier option. The value $\Pi$ of a portfolio of $N$ options can be seen as the sum of the option prices:

$$
\Pi(t) = \sum_{i=1}^{N} U_i(S_t, K_i, T_i), \tag{32}
$$

where $K_i$ is the strike, $T_i$ the maturity and $U_i$ the price of option $i$. In this paper option $i$ can thus be a European call or put option, or a barrier option. We assume that all options in the portfolio can be netted.

Together with the Monte Carlo scenario generation, this gives us the exposure profile of the sum of the option values at any future time point. The duration of the portfolio is equal to the longest maturity in the portfolio:

$$\tilde{T} = \max_{i \in [1,N]} T_i. \tag{33}$$

Again, at this maximum maturity, all the option prices on the grid are known, therefore the time is reversed such that the payoff formula (34) can be used as an initial condition which equals the sum of all individual payoff functions belonging to options with maturity equal to the maximum maturity $\tilde{T}$.

$$\phi_P(S_t) = \sum_{i=1}^{M} \phi_i(S_t, K_i, T_i) \mathbb{1}_{\{T_i = \tilde{T}\}}. \tag{34}$$

Important in the context of this research is that the option specific characteristics are only introduced by the initial condition and the boundary conditions. Because the portfolio consists of a sum of options, the boundary conditions for the portfolio will also be just a sum of these limiting conditions, such that our time stepping routine in the finite difference procedure can be updated as follows:

- From $\boldsymbol{u}^n$, calculate $\boldsymbol{u}^{n-1}$ by the ADI splitting scheme
- update the portfolio value with possible other option values:

  $$\boldsymbol{u}^{n-1} = \boldsymbol{u}^{n-1} + \sum_{i=1}^{M} \phi_i(\vec{S}, K_i, T_i) \mathbb{1}_{\{T_i = t_{n-1}\}},$$

  where $\boldsymbol{s}$ is a vector of the same size as $\boldsymbol{u}$ consisting of all $S$ grid points.
- update all boundary conditions

Such that at $\boldsymbol{u}^0$ equals the value of the portfolio at time $t = t_0$. For the computation of exposure of a portfolio over time, can only include all options that are not path-dependent, on one grid. For path dependent options, a routine is needed to check if options are exercised. In the case of a portfolio of a call, put and a barrier considered in this research. The EE of the call and put option are computed using only one grid, whereas the EE of the barrier option is computed using the algorithm from section 3.1.

# 4 Numerical Results

## 4.1 Single barrier options: Numerical Setup

Computing the exposure of barrier options is more challenging than computing the exposure of European options. Barrier options are path dependent and have a discontinuous initial condition. Especially this discontinuous nature of the payoff function may complicate accurate estimation of sensitivities, particularly the higher-order ones. Because we have a benchmark solution for Down-and-Out Put (DOP) options, we do an extensive error analysis for this option type,

Table 2: Model parameters for various test cases.

| | Case A | Case B |
|---|---|---|
| Spot ($S_0$) | 1.364 | 138.1 |
| Domestic short rate ($r^d$) | 0.01 | 0.03 |
| Foreign short rate ($r^f$) | 0.01 | 0.10 |
| Initial variance ($v_0$) | 0.029 | 0.029 |
| Mean reversion speed ($\kappa$) | 4.42 | 1.50 |
| Mean reversion level ($\eta$) | 0.0240 | 0.0707 |
| Vol of vol ($\sigma$) | 0.46 | 0.63 |
| Correlation ($\rho$) | -0.45 | -0.76 |
| Maturity ($T$) | 0.5 | 1.0 |
| Strike ($K$) | 1.360 | 138.1 |
| Barrier ($B$) | 1.20 | 120 |

but the method can also be applied to Down-and-Out Call (DOC), Up-and-Out Put (UOP) and Up and Out Call (UOC) options.

The parameters are chosen according to table 2. In test A the foreign interest rate is equal to the domestic rate, next to that the option is Out - of - The - Money (OTM) at inception. The level of the initial FX rate is set at 1.3639, which is a real market quoted EUR/USD FX rate from June 2014, whereas the other parameters satisfy characteristics observed in literature, such as negative correlation, low volatility and small maturities (see eg, Schoutens et al. (2004) and Albrecher et al. (2007)). In this test, the well known Feller condition is satisfied. In test B the initial FX rate is set to 138.1, a real EUR/JPY FX rate from June 2014, the option is OTM at inception while the domestic rate is higher than the foreign rate. In this case the other model parameters are chosen such that the Feller condition is violated.[2]

## 4.2 Accuracy and Convergence

The computed EE, $\text{PFE}_{2.5\%}$ and $\text{PFE}_{97.5\%}$ are shown in figures 2(a) and 2(b). The starting level of the EE, equals the option price at $t = t_0$ and shows a small increase towards maturity. The PFE however, shows a more interesting behavior. Starting at the option price, the PFE is increasing over time and shows a steep growth close to maturity. Intuitively the increase of the higher quantile makes sense, when moving $t^* \in [t_0, T]$ closer to maturity, the hitting probability conditioned on no prior barrier hit, will become smaller, such that for in - the - money paths, the price will resemble more and more a straightforward European option value. The mean (EE) is not heavily effected because also the probability of the barrier being hit up to time $t^*$ is increased which will lower the option value.

As a benchmark, the COS method can be applied to evaluate barrier options accurate and efficient. For details on the pricing procedure using this Fourier cosine method we refer to Fang and Oosterlee (2011). Here we use this efficient pricing technique by computing prices for an entire grid of possible market

[2]When the Feller condition is not satisfied, the variance process can become zero and numerical methods can become unstable.

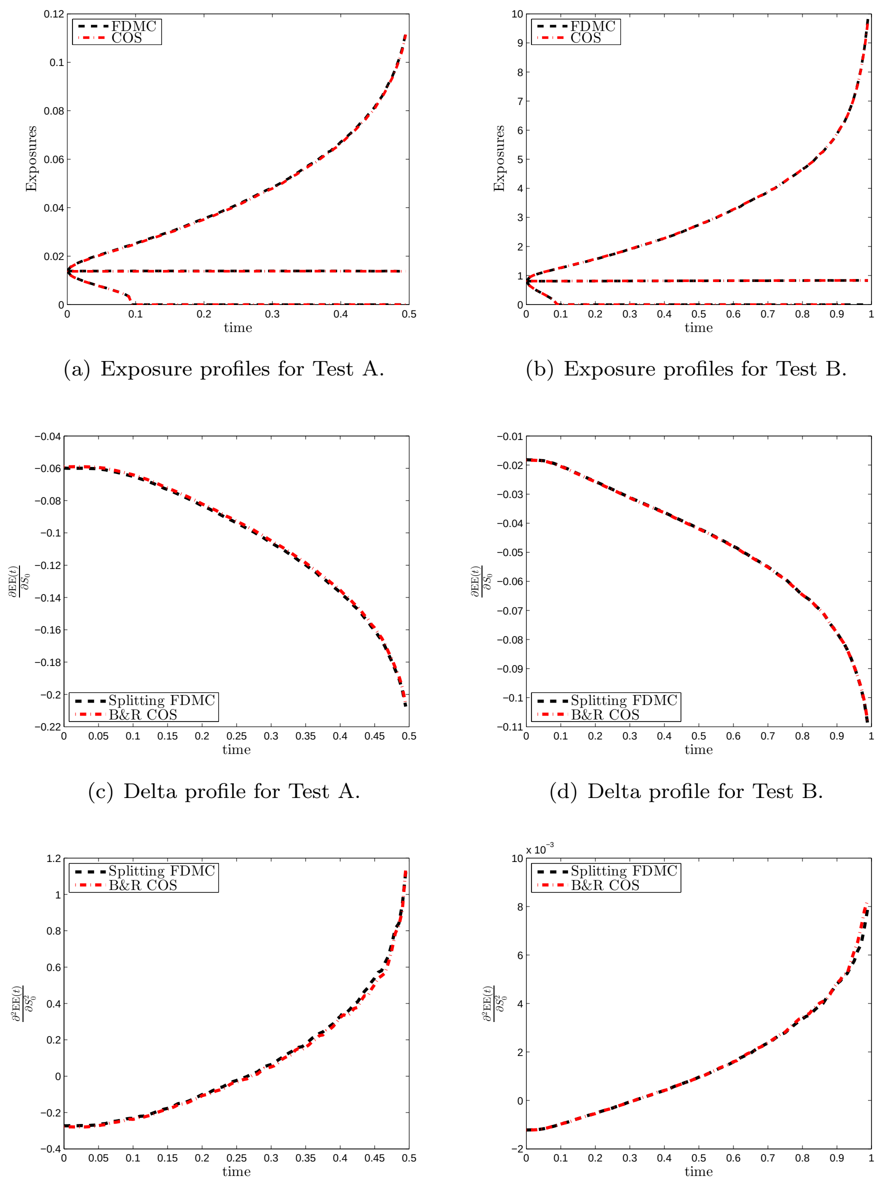


(a) Exposure profiles for Test A.

(b) Exposure profiles for Test B.

(c) Delta profile for Test A.

(d) Delta profile for Test B.

(e) Gamma profile for Test A.

(f) Gamma profile for Test B.

Figure 2: Exposures (EE, $\mathrm{PFE}_{2.5\%}$ and $\mathrm{PFE}_{97.5\%}$) and the first and second derivative profiles over time under the Heston dynamics for tests A and B. The dashed black line is computed using the FDMC method, whereas the dashed red line is computed using the COS method. In the case of the sensitivities, the results corresponding to the COS method are obtained using a Bump-and-Revalue (B&R) procedure whereas for the FDMC method the derivative is splitted as explained in section 3.3.

Table 3: Relative $L_2$ and $L_\infty$ errors compared to the COS method using the linear or spline interpolation.

| | | Linear interpolation | | Spline interpolation | |
|---|---|---|---|---|---|
| Error | Quantity | Test A | Test B | Test A | Test B |
| $\|\|\cdot\|\|_\infty$ | EE | $2.1728\ 10^{-3}$ | $3.7094\ 10^{-3}$ | $2.1690\ 10^{-3}$ | $3.7006\ 10^{-3}$ |
| | $\text{PFE}_{97.5\%}$ | $4.9120\ 10^{-3}$ | $5.3274\ 10^{-3}$ | $4.9213\ 10^{-3}$ | $5.2280\ 10^{-3}$ |
| | $\frac{\partial \text{EE}}{\partial S_0}$ | $4.7905\ 10^{-3}$ | $6.6173\ 10^{-3}$ | $4.8058\ 10^{-3}$ | $6.6243\ 10^{-3}$ |
| | $\frac{\partial^2 \text{EE}}{\partial S_0^2}$ | $3.5990\ 10^{-2}$ | $3.7086\ 10^{-2}$ | $3.5982\ 10^{-2}$ | $3.7107\ 10^{-2}$ |
| $\|\|\cdot\|\|_2$ | EE | $1.8225\ 10^{-3}$ | $3.1294\ 10^{-3}$ | $1.8197\ 10^{-3}$ | $3.1216\ 10^{-3}$ |
| | $\text{PFE}_{97.5\%}$ | $3.0751\ 10^{-3}$ | $5.2244\ 10^{-3}$ | $3.0832\ 10^{-3}$ | $5.2280\ 10^{-3}$ |
| | $\frac{\partial \text{EE}}{\partial S_0}$ | $3.8470\ 10^{-3}$ | $5.3315\ 10^{-3}$ | $3.8508\ 10^{-3}$ | $5.2280\ 10^{-3}$ |
| | $\frac{\partial^2 \text{EE}}{\partial S_0^2}$ | $2.5988\ 10^{-2}$ | $2.2843\ 10^{-2}$ | $2.5921\ 10^{-2}$ | $2.2881\ 10^{-2}$ |

scenarios. Similar as the grid used for the finite difference procedure, this grid is chosen large enough to contain all future market scenarios generated by the Monte Carlo scenario generation. We choose 500 points in $S$ - and 300 points in $V$ - direction, both densely distributed around the expected means. Prices for all the scenarios are obtained by a spline interpolation on the COS grid.

For the sensitivities, we run this procedure two (in the case of delta) or three (in the case of gamma) times with an initial condition bumped by $\epsilon$. From the results, the sensitivities are computed by the finite difference formulas:

$$\frac{\partial \text{EE}(t)}{\partial S_0} \approx \frac{\text{EE}_{S_0+\epsilon}(t) - \text{EE}_{S_0-\epsilon}(t)}{2\epsilon}, \tag{35}$$

$$\frac{\partial^2 \text{EE}(t)}{\partial S_0^2} \approx \frac{\text{EE}_{S_0+\epsilon}(t) - 2\text{EE}_{S_0}(t) + \text{EE}_{S_0-\epsilon}(t)}{\epsilon^2}. \tag{36}$$

Figures 2(a) to 2(f) show that the exposure profiles and sensitivities over time computed with the FDMC method resemble the results computed by the Monte Carlo COS method.

For an EE computed over $N_T$ evaluation dates, the relative $L_2$ and $L_\infty$ errors are computed as:

$$||\cdot||_\infty := \max_{i=1,\dots,N_T} \left|\text{EE}_i^{\text{COS}} - \text{EE}_i^{\text{FDMC}}\right| \Big/ \max_{i=1,\dots,N_T} \left|\text{EE}_i^{\text{COS}}\right|, \tag{37}$$

$$||\cdot||_2 := \left(\sum_{i=1}^{N_T} \left(\text{EE}_i^{\text{COS}} - \text{EE}_i^{\text{FDMC}}\right)^2\right)^{\frac{1}{2}} \Bigg/ \left(\sum_{i=1}^{N_T} \left(\text{EE}_i^{\text{COS}}\right)^2\right)^{\frac{1}{2}}. \tag{38}$$

In table 3 the errors between the FDMC method with 700 grid points in $S$ - and 350 in $V$ -direction are compared to the COS method. We can see that the relative error is below 1% in both EE and the first derivative. The second derivative however, is accurate up to 5% in both $L_\infty$ and $L_2$ norm. This is due to the fact that this absolute value of gamma is already in the range of $10^{-4}$ such that the errors from the finite difference discretization have a larger impact. Furthermore, we can see that the difference between a spline and linear interpolation is negligible.

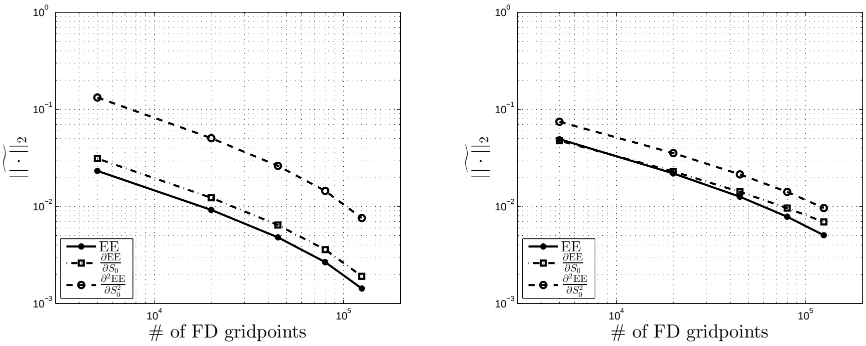


(a) Test A (b) Test B

Figure 3: Error convergence of EE and first - and second - order sensitivities for tests A and B by increasing the number of grid points ($2m \times m$) used in the finite difference computation. We use $m$ in $V$ - and $2m$ in $S$ -direction. For every exposure computation, $10^5$ paths are used simulated with a fixed seed to avoid noise. Here, a spline interpolation is used, but similar analysis performed using a linear interpolation is shown in table 3.

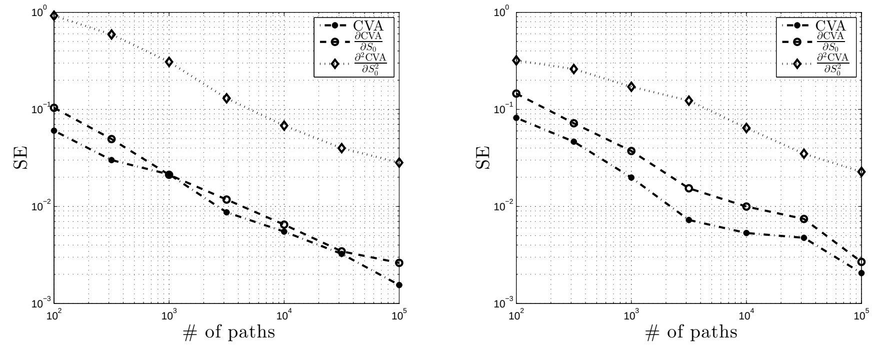


(a) Test A (b) Test B

Figure 4: Convergence of the relative Standard Error (SE) of CVA, delta of CVA and gamma of CVA for tests A and B for increasing number of paths. Here, the number of finite difference grid points is set equal to 350 in $V$ - and 700 in $S$ - direction and the standard error is computed relative to the mean.

Table 4: The change of price, delta and gamma by adding CVA to barrier options for various moneyness levels. The significant numbers are computed up to 1% for CVA and delta and 5% for gamma due to the standard deviation.

| | Quantity | OTM $K = 0.9S_0$ | ATM $K = S_0$ | ITM $K = 1.1S_0$ |
|---|---|---|---|---|
| Test A | CVA | 1.99% | 2.00% | 1.99% |
| | Delta | 4.70% | 3.47% | 3.66% |
| | Gamma | -15 % | -0.39% | 1.5% |
| Test B | CVA | 3.96% | 3.98% | 3.98% |
| | Delta | 16.75% | 9.96% | 13.3% |
| | Gamma | -13 % | -5.1% | 2.0% |

The convergence with respect to the number of finite difference grid points is shown in figures 3(a) and 3(b), for the EE and the first and second derivative with respect to $S_0$. In this case, the benchmark is the converged finite difference solution obtained with 700 and 350 points in $S$ - and $V$ - direction respectively. The convergence is shown to be first - order in the number of grid points.

In figures 4(a) and 4(b), we show the decline of the relative Standard Error (SE) in percentage of the mean, by increasing the number of paths for tests A and B. Here we computed this standard error using 10 Monte Carlo simulations with different seeds. Typically, the Monte Carlo convergence is expected to be $1/\sqrt{N_p}$ where $N_p$ is the number of Monte Carlo paths. We see that for both tests, all quantities converge as expected.

## 4.3 CVA and sensitivities for barrier options

For the evaluation of CVA, we assume a recovery rate of 40%. The hazard rate is computed by assuming a 5 year CDS with a spread of 400 basis points paid quarterly. The Euro discount factors are taken from April 2014, the resulting survival probabilities up to one year are obtained as explained in section 3.3. Because we assume absence of wrong - and right - way risk, we can compute the CVA for any CDS spread. In this case, CVA is a linear function of the CDS spread.

To investigate the barrier effect on CVA, we compute CVA and its sensitivities as a function of the barrier level, in figure 5. The strike is set at - the - money ($S_0 = K$) and for barriers lower then $K$ we look at Down - and - Out Put (DOP) options, while for barriers higher than strike we compute Up - and - Out Call (UOC) options. As expected for barrier options with a barrier close to strike, the CVA as well as the sensitivities decrease to zero.

To further investigate the impact of the CVA and its sensitivities we look at the difference between the measures with and without CVA adjustment:

$$
\begin{aligned}
U^* &= U + \text{CVA},\\
\frac{\partial U^*}{\partial S_0} &= \frac{\partial U}{\partial S_0} + \frac{\partial \text{CVA}}{\partial S_0},\\
\frac{\partial^2 U^*}{\partial S_0^2} &= \frac{\partial^2 U}{\partial^2 S_0} + \frac{\partial^2 \text{CVA}}{\partial S_0^2}.
\end{aligned}
$$

In table 4 we show the impact of CVA on the option price and its sensitivities.

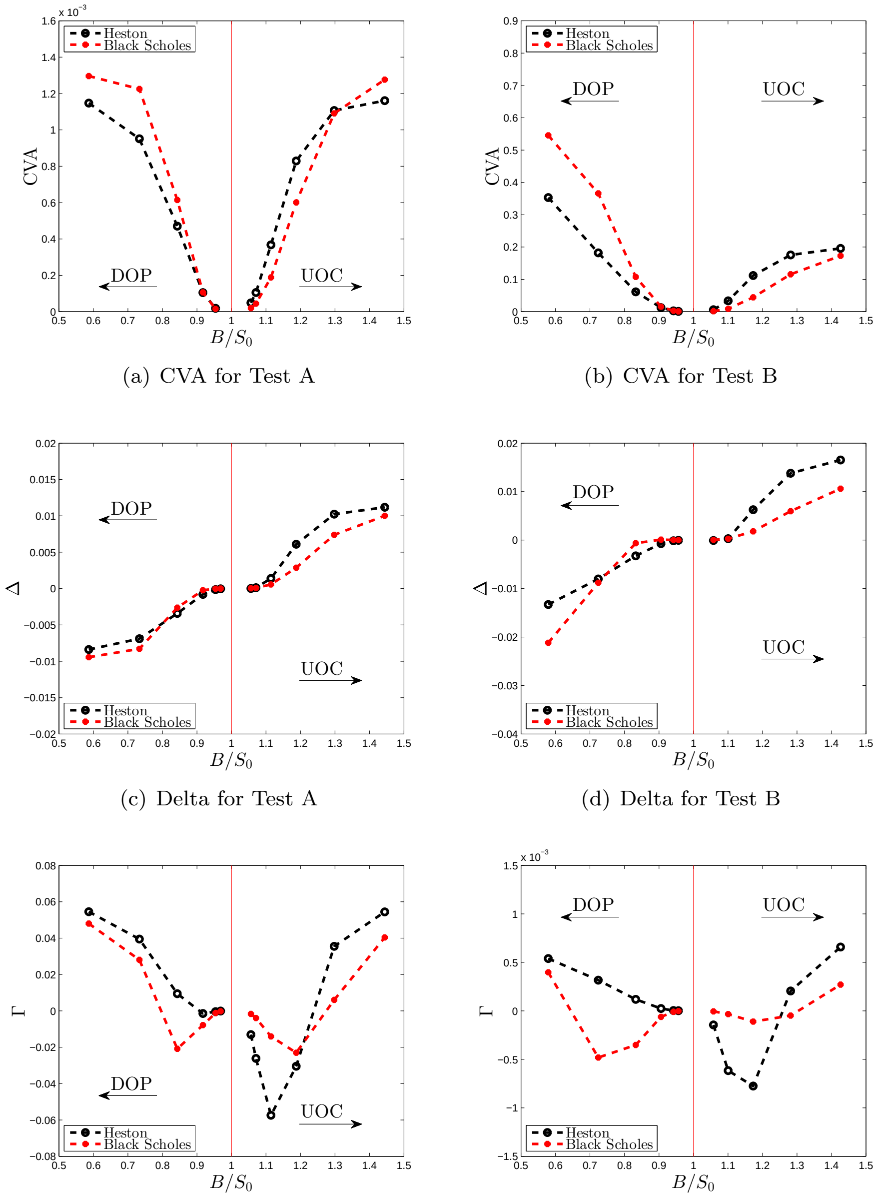


(a) CVA for Test A

(b) CVA for Test B

(c) Delta for Test A

(d) Delta for Test B

(e) Gamma for Test A

(f) Gamma for Test B

Figure 5: CVA as a function of the barrier level. The CVA is calculated assuming a LGD of 40% and a fixed CDS spread of 400 basis points. The number of paths is equal to 100.000 and for the FD computation we take 250 grid points in $V$ - and 500 grid points in $S$ - direction. The standard error is less then 3% for all barrier levels.

Table 5: Tested portfolios.

| | | Type | Maturity | Strike | Barrier |
|---|---|---|---|---|---|
| Portfolio I | Option 1 | Call | $T_1 = 1$ | $K_1 = 133$ | - |
| | Option 2 | Put | $T_2 = 0.4$ | $K_2 = 138$ | - |
| | Option 3 | Barrier | $T_3 = 0.8$ | $K_3 = 135$ | $B_3 = 120$ |
| Portfolio II | Option 1 | Call | $T_1 = 1$ | $K_1 = 133$ | - |
| | Option 2 | Put | $T_2 = 0.4$ | $K_2 = 138$ | - |

The CVA delta and gamma are quoted as percentages of the risk - free valuation ($U$) where no CVA is charged. We can conclude that, for different moneyness levels, the CVA adjustment is stable, but the delta and gamma differ significant. Furthermore, figures 5(a) to 5(f) show that the impact of skew on CVA and its sensitivities can not be ignored. Results for gamma computed assuming the Heston dynamics or the Black - Scholes dynamics can even differ in sign.

## 4.4 Portfolio of options

Different options in one portfolio can have different strikes and maturities. Due to these different maturities, the finite difference procedure is faced with a discontinuity in time. To assess the possible effect on the accuracy, we consider a portfolio of two European options with different strike and maturity. We again compare the resulting exposure profiles and CVA values with the Monte Carlo COS method. For the benchmark, we compute separate exposure profiles for every option with the Monte Carlo COS method and compute the EE of the portfolios as the sum. This is similar for the sensitivities that are obtained by a bump - and - revalue procedure per option. In the FDMC method, the Call and Put option are computed simultaneously on one grid. The barrier option is computed on a separate grid because for every path termination needs to be checked. The resulting option prices per path are added to the portfolio values and from this, the mean and quantiles can be calculated.

Again we assume the Heston dynamics to drive the underlying risk factors. The Heston parameters that drive the underlying are chosen as in case B of the previous subsection. All the options in the portfolio are written on this single FX rate. We consider two portfolios. Portfolio I consists of a call, put and a barrier option, while portfolio II consists only of the call and a put. Table 5 shows the option parameters for the two portfolios.

The results presented in this paper also hold for portfolios consisting of an arbitrary larger number of options, but for illustrative reasons we present results for only three options.

In table 6 we show the CVA values. Here we computed the CVA as a percentage of the portfolio value. The sensitivities are quoted relative to the sensitivities of the initial portfolio. This way we can quantify the change between

Table 6: CVA, delta and gamma for the portfolios I and II as a percentage of non-adjusted values. The percentages are computed by spline and linear interpolation both for the FDMC method as for the benchmark COS method. The sensitivities in the COS method are obtained by a bump and revalue technique.

| | Linear interpolation | | Spline interpolation | |
|---|---|---|---|---|
| | Portfolio I | Portfolio II | Portfolio I | Portfolio II |
| CVA FDMC | 2.79% | 2.77% | 2.79% | 2.77% |
| CVA COS | 2.79% | 2.77% | 2.79% | 2.77% |
| $\Delta_{S_0}$ Splitting FDMC | 23.49% | 18.78% | 23.29% | 18.72% |
| $\Delta_{S_0}$ B&R COS | 23.52% | 18.85% | 23.40% | 18.79% |
| $\Gamma_{S_0}$ Splitting FDMC | 2.58% | 2.42% | 2.57% | 2.41% |
| $\Gamma_{S_0}$ B&R COS | 2.52% | 2.38% | 2.57% | 2.43% |

the CVA adjusted and the non CVA adjusted portfolio:

$$\mathrm{CVA}_{\%} := 100\frac{\mathrm{CVA}}{\Pi}, \tag{39}$$

$$\Delta_{S_0} := 100\frac{\partial \mathrm{CVA}}{\partial S_0} \Big/ \frac{\partial \Pi}{\partial S_0}, \tag{40}$$

$$\Gamma_{S_0} := 100\frac{\partial^2 \mathrm{CVA}}{\partial S_0^2} \Big/ \frac{\partial^2 \Pi}{\partial S_0^2}. \tag{41}$$

By looking at figures 6(a) and 6(b), we can see that the EE drops at $t = 0.4$ when the put option expires. This discontinuity is captured nicely by the FDMC method, where the put and call option are computed on one finite difference grid. By looking at table 6 we can conclude that the resulting value adjustments are accurate compared to the Monte Carlo COS method. Next to that the difference between spline and linear interpolation is small.

In portfolio I, the call and put option have a bigger effect on the EE than the barrier option. Also the higher PFE is heavily affected by the expiry of the put option. If we compare figures 6(a) and 6(b) we can see that the impact of the expiring barrier option at $T = 0.8$ is not reflected in the PFE and only minor in the EE profile. This minor barrier effect is also visible when we compare the CVAs for portfolio I and II. The difference between these portfolios is due to the barrier option and we can see a CVA difference of 1.5% in table 6.

Next, if we look at the delta profiles in figures 6(c) and 6(d), we see that for portfolio I, the impact of the barrier option is reflected by a steep decrease at the expiry of the barrier option $T = 0.8$. As this barrier option is absent in portfolio II, this decrease is absent in the delta profile of portfolio II. This impact is also confirmed by looking at the sensitivity of CVA with respect to $S_0$ in table 6 where the difference between portfolio I and II is in the range of 25% for $\Delta_{S_0}$.

In the case of gamma, shown in figures 6(e) and 6(f), the barrier option in portfolio I shows a steep increase at the expiry of the barrier option. The relative impact for gamma however is smaller than for delta, as in table 6, we see that the difference in gamma between portfolio I and II is in the range of 3%.

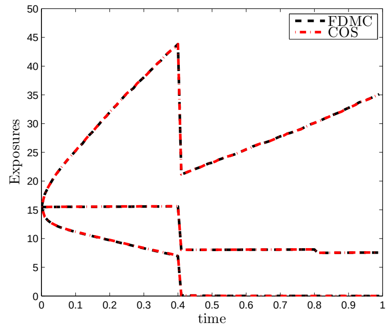


(a) Exposure profiles for portfolio I.

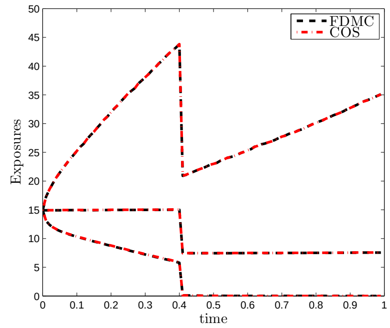


(b) Exposure profiles for portfolio II.

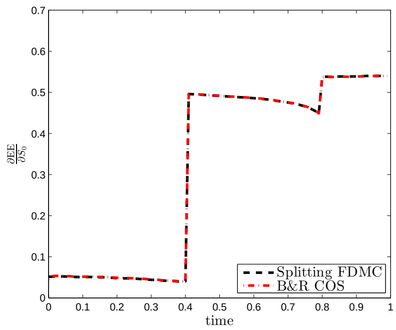


(c) Delta profile for portfolio I.

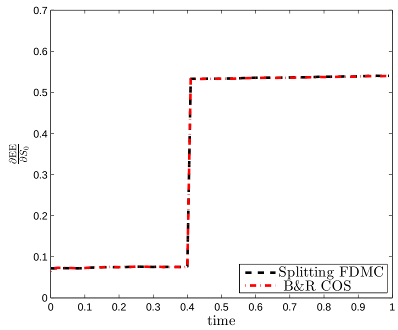


(d) Delta profile for portfolio II.

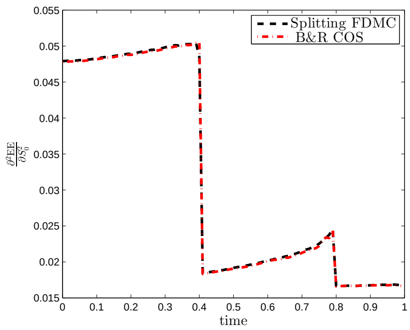


(e) Gamma profile for portfolio I.

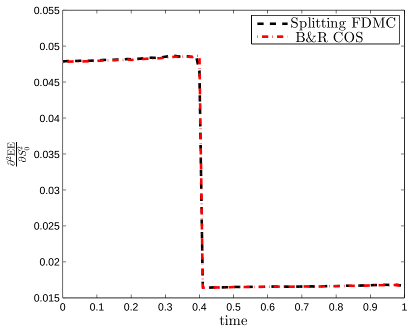


(f) Gamma profile for portfolio II.

Figure 6: Exposure, Delta and Gamma profiles for portfolios I and II over time for Case B computed with the FDMC method or with the COS method. Again the COS sensitivities are computed running 2 or three simulations from a bumped initial value. The results results compared to the COS method are acurate up to an order of $10^{-3}$.

We can furthermore see that the spline interpolation yield similar results as the linear interpolation. These results indicate that the effect of a barrier options in a portfolio can be more severe in the sense of sensitivities than in CVA itself. Clearly, a small chnage in the EE profile can have a bigger impact on the first - and second - order sensitivity.

# 5 Conclusion

In this research we propose a new computational technique to compute Exposure profiles and its sensitivities. This paper extends the FDMC method described in de Graaf et al. (2014) and is based on combining the Monte Carlo scenario generation with option valuation by solving a PDE on a grid. For every scenario at every time point the option prices are obtained by interpolating the scenarios on this option grid. The Expected Exposure needed for the computation of CVA is computed by averaging. We have shown that the FDMC is a computationally efficient and accurate method compared to a benchmark Monte Carlo COS method and can therefore serve as an alternative to the widely used American Style Monte Carlo approach, which in application to exotic options can suffer from regression bias.

The sensitivities are obtained efficiently by leveraging from the finite difference grid. Compared to a 'brute force' bump - and - revalue technique the sensitivity results are accurate and no extra Monte Carlo simulations are needed such that the computation time is less. We analyze the accuracy of the method by comparing with a benchmark solution and we asses the convergence of the solutions by first increasing the number of paths in the Monte Carlo simulation and secondly, increasing the number of grid points used in the finite difference procedure. As expected, the standard error converges by $1 \big/ \sqrt{N}$, where N is the number of paths. By increasing the number of grid points, the relative error converges in first order. Also the effect of the interpolation is studied, for all tests considered, a straightforward linear interpolation shows to be sufficient.

Next we show that we can use the method to compute exposure profiles for a portfolio of options with different maturities. In this portfolio, the EEs of all options that are not path dependent (European options) can be efficiently computed on a single grid. The resulting discontinuity in time is captured and no significant error propagation is observed. The EEs for path dependent options have to be computed individually, but can be added to the portfolio before computing the means. The sensitivities can again be computed with small extra computational time. Results compared to the Monte Carlo COS method are again accurate, as well as for linear as for spline interpolation. Next to that, the impact of including a relatively 'cheap' barrier option to a portfolio consisting of a relatively 'expensive' call and put option, might have a small CVA impact, but can have a more severe effect on the first and second order sensitivity of the portfolio.

In a forthcoming research we assess in detail the effect of skew and stochastic interest rate on CVA and its sensitivities by using model parameters calibrated to real market data and a wide range of option contract parameters.

## Acknowledgments

This work was supported by the Dutch Technology Foundation STW under project 12214. Peter Sloot acknowledges support from the Russian Scientific foundation, grant 14 - 21 - 00137. We would like to thank Qian Feng for helpful advice regarding the Monte Carlo COS method. Furthermore we thank Norbert Hari, Shashi Jain and Sarunas Simaitis for fruitful discussions about the FDMC method.


# A Interest rate sensitivity

If we assume the interest rate to be stochastic, it is important to measure the sensitivity with respect to the initial domestic short rate $r_0^d$. As a consequence, the EE now also depends on the stochastic interest rate, but we still assume that the exposure and the counterparties default probability are independent. Using this, we can formulate the expression for credit valuation adjustment (CVA) as follows Gregory (2010):

$$\mathrm{CVA}(0,T) = (1-R)\int_0^T \mathbb{E}\left[D(0,t_k)\mathrm{E}(t_k)|\mathcal{F}_0\right] dPD(t), \tag{42}$$

where $\mathrm{EE}(t_k) := \mathbb{E}\left[D(0,t_k)\mathrm{E}(t_k)|\mathcal{F}_0\right]$ equals the expected current (discounted) value of the future exposure at time $t_k$. Now, in a discrete setting CVA, with a recovery rate $R$ set to zero for notational convenience, can be calculated as:

$$\mathrm{CVA} = \sum_{k=1}^{N} q(t_{k-1},t_k)\mathrm{EE}(t_k), \tag{43}$$

where in this case, $\mathrm{EE}(t_k)$ is a function of $r_t^d, V_t$ and $S_t$. For the derivative with respect to the initial interest rate, we thus have:

$$\begin{aligned}
\frac{\partial \mathrm{CVA}}{\partial r_0^d} &= \frac{\partial}{\partial r_0^d}\sum_{k=1}^{N} q(t_{k-1},t_k)\mathrm{EE}(t_k), && (44)\\
&= \sum_{k=1}^{N} q(t_{k-1},t_k)\frac{\partial \mathrm{EE}(t_k)}{\partial r_0^d}, && (45)\\
&= \sum_{k=1}^{N} q(t_{k-1},t_k)\left(\frac{\partial \mathrm{EE}(t_k)}{\partial S_{t_k}}\frac{\partial S_{t_k}}{\partial r_0^d} + \frac{\partial \mathrm{EE}(t_k)}{\partial V_{t_k}}\frac{\partial V_{t_k}}{\partial r_0^d} + \frac{\partial \mathrm{EE}(t_k)}{\partial r_{t_k}^d}\frac{\partial r_{t_k}^d}{\partial r_0^d}\right) && (46)\\
&= \sum_{k=1}^{N} q(t_{k-1},t_k)\left(\frac{\partial \mathrm{EE}(t_k)}{\partial S_{t_k}}\frac{\partial S_{t_k}}{\partial r_0^d} + \frac{\partial \mathrm{EE}(t_k)}{\partial r_{t_k}^d}\frac{\partial r_{t_k}^d}{\partial r_0^d}\right). && (47)
\end{aligned}$$

Where the future volatility is independent of $r_0^d$, such that the second expression in (46) equals zero. Similar as in the case of the Heston model, the local derivatives of the EE can be derived from the finite difference grid. At every intermediate time point $t_k$, the finite difference method stores the prices for the entire grid in the vector $\boldsymbol{u}^k = \boldsymbol{u}(t_k) = \mathrm{EE}(t_k)$. On this grid we can approximate

$\frac{\partial \mathrm{EE}(t_k)}{\partial S_{t_k}}$ and $\frac{\partial \mathrm{EE}(t_k)}{\partial r_{t_k}}$ by multiplying with the difference matrix $\mathbf{A}_S$ or $\mathbf{A}_r(t_k)$[3] respectively:

$$\frac{\partial \boldsymbol{u}(t_k)}{\partial S} \approx \mathbf{A}_S \boldsymbol{u}^k = \frac{\partial \boldsymbol{u}(t_k)}{\partial S} + \mathcal{O}(\Delta s^2). \tag{48}$$

$$\frac{\partial \boldsymbol{u}(t_k)}{\partial r^d_{t_k}} \approx \mathbf{A}_r(t_k) \boldsymbol{u}^k = \frac{\partial \boldsymbol{u}(t_k)}{\partial r^d_{t_k}} + \mathcal{O}((\Delta r^d)^2). \tag{49}$$

The partial derivatives of the state variables with respect to $r^d_0$, can be computed along the path in the Monte Carlo simulation. Let $t_k$ $(0 < k < N)$ be a discrete simulation time in $0 = t_0, \ldots, t_N$. Then, we can create a recursive formula for $\frac{\partial S_{t_k}}{\partial r^d_0}$:

$$\frac{\partial S_{t_k}}{\partial r^d_0} = \frac{\partial S_{t_k}}{\partial S_{t_{k-1}}} \frac{\partial S_{t_{k-1}}}{\partial r^d_0} + \frac{\partial S_{t_k}}{\partial r_{t_{k-1}}} \frac{\partial r^d_{t_{k-1}}}{\partial r^d_0}, \tag{50}$$

where, when $S_t$ is driven by a geometric Brownian motion, we have:

$$\frac{\partial S_{t_k}}{\partial S_{t_{k-1}}} = \frac{S_{t_k}}{S_{t_{k-1}}}, \tag{51}$$

$$\frac{\partial S_{t_k}}{\partial r^d_{t_{k-1}}} = S_{t_k} \Delta t, \tag{52}$$

where $\Delta t = t_k - t_{k-1}$ is the uniform time increment in one time step. Furthermore, when the interest rate is modeled by the Hull - White model (Hull and White (1993)):

$$dr^d_t = \lambda^{r^d} \left[\theta^d(t) - r^d_t\right] dt + \sigma^r \, dW(t), \tag{53}$$

where $\lambda^d_{r^d}$ is the mean reverting speed, $\theta^d(t)$ the mean reverting level and $\sigma^r$ the instantaneous volatility. Using an Euler scheme as a discretization yields:

$$r^d_{t_{k+1}} = r^d_{t_k} + \lambda^{r^d} \left[\theta^d(t_k) - r^d_{t_k}\right] \Delta t + \sigma^r \sqrt{\Delta t} Z_{t_k}, \tag{54}$$

Where $Z$ $N(0,1)$. From this we can recursively derive:

$$\frac{\partial r_{t_{k-1}}}{\partial r^d_0} = (1 - \lambda^d_{r^d} \Delta t)^{(k-1)}. \tag{55}$$

The first time step gives us the initial condition:

$$\frac{\partial S_{t_1}}{\partial r^d_0} = S_0 \Delta t. \tag{56}$$

Using this recursive formula together with the finite difference approximations, we can estimate the future derivative with respect to $r^d_0$ without the need of an extra Monte Carlo simulation. So to summarize, for the computation of the sensitivity of CVA with respect to interest rate, we need:

[3] Note that $\mathbf{A}_r(t_k)$ is a time dependent matrix, as in the case of stochastic interest rate, the drift can be time dependent because of the yield curve, see eg, the Hull - White model

- $\frac{\partial \text{EE}(t_k)}{\partial S_{t_k}}$, can be obtained from finite difference grid,
- $\frac{\partial \text{EE}(t_k)}{\partial r^d_{t_k}}$, can be obtained from finite difference grid,
- $\frac{\partial r^d_{t_k}}{\partial r^d_0}$, is model dependent, but can be obtained analytically for Hull - White.

Choosing similar parameters as in Case B from section 4 with the following added interest rate parameters:

$$\lambda^{r^d} = 0.5, \qquad \theta^d(t) = 0.05, \qquad \sigma^r = 0.02 \qquad \rho_{S,r^d} = -0.01, \tag{57}$$

for a European call option with strike $K = 120$ and maturity $T = 1$ we get the profile for $\frac{\partial \text{EE}(t_k)}{\partial r^d_0}$ as presented in figure 7.

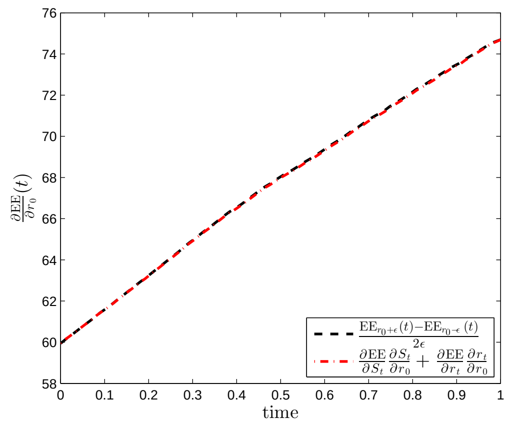


Figure 7: The sensitivity of the Exposure of a European call option over time with respect to intial interest rate $r^d_0$. Note that in this case, the domestic interest rate $r^d_t$ is modeled by the Hull - White model. The foreign interest rate is deterministic.

# References


Albrecher, H., P. Mayer, W. Schoutens, and J. Tistaert (2007). The little Heston trap. *Wilmott Mag., January*, 83–92.

Andersen, L. (2008). Simple and efficient simulation of the Heston stochastic volatility model. *Journal of Computational Finance 11*(3), 1–42.

Basel Committee on Banking Supervision (2010). Basel III: A global regulatory framework for more resilient banks and banking systems. Technical Report June.

Broadie, M. and P. Glasserman (1996). Estimating security price derivatives using simulation. *Management science 42*(2), 269–285.

de Graaf, C. S. L., Q. Feng, B. D. Kandhai, and C. W. Oosterlee (2014). Efficient Computation of Exposure Profiles for Counterparty Credit Risk. *International Journal of Theoretical and Applied Finance 17*(4), 1–24.

Ekström, E. and J. Tysk (2011, February). Boundary conditions for the single-factor term structure equation. *The Annals of Applied Probability 21*(1), 332–350.

Fang, F. and C. W. Oosterlee (2011, January). A Fourier-Based Valuation Method for Bermudan and Barrier Options under Heston's Model. *SIAM Journal on Financial Mathematics 2*(1), 439–463.

Gregory, J. (2010). *Counterparty Credit Risk*. Wiley Online Library.

Haentjens, T. and K. J. in 't Hout (2012). ADI finite difference schemes for the Heston–Hull–White PDE. *Journal of Computational Finance 16*(1), 83–110.

Heston, S. L. (1993). A Closed-Form Solution for Options with Stochastic Volatility with Applications to Bond and Currency Options. *The Review of Financial Studies 6*(2), 327–343.

Hull, J. and A. White (1993). One-factor interest-rate models and the valuation of interest-rate derivative securities. *Journal of Financial and Quantitative Analysis 28*(2), 235–254.

Hundsdorfer, W. and J. G. Verwer (2003). *Numerical Solution of Time-Dependent Advection-Diffusion-Reaction Equations*, Volume 33.

in 't Hout, K. J. and S. Foulon (2010). ADI Finite Difference Schemes For Option Pricing. *International Journal of Numerical Analysis and Modeling 7*(2), 303–320.

in 't Hout, K. J. and B. D. Welfert (2009, March). Unconditional stability of second-order ADI schemes applied to multi-dimensional diffusion equations with mixed derivative terms. *Applied Numerical Mathematics 59*(3-4), 677–692.

Ng, L. and D. Peterson (2009, August). Potential future exposure calculations using the BGM model. *Wilmott Journal 1*(4), 213–225.

Ng, L., D. Peterson, and A. E. Rodriguez (2010). Potential future exposure calculations of multi-asset exotic products using the stochastic mesh method. *Journal of Computational Finance 14*(2).

Schoutens, W., E. Simons, and J. Tistaert (2004). A perfect calibration! Now what? *Wilmott Mag., March*, 66–78.

Shen, Y., J. A. M. Weide, and J. H. M. Anderluh (2013). A Benchmark Approach of Counterparty Credit Exposure of Bermudan Option under Lévy Process: The Monte Carlo-COS Method. *Procedia Computer Science 18*, 1163–1171.

Tavella, D. and C. Randall (2000). *Pricing Financial Instruments: The Finite Difference Method*. New York: Wiley.

Whetten, M., M. Adelson, and M. V. Bemmelen (2004). Credit Default Swap (CDS) Primer. *Nomura Fixed Income Research* (April), 1–12.